



Next-generation sequencing implicates oncogenic roles for p53 and JAK/STAT signaling in microcystic adnexal carcinomas

May P. Chan ^{1,2,3} · Komal R. Plouffe^{1,4,5} · Chia-Jen Liu^{1,4} · Nallasivam Palanisamy ⁶ · Shannon Carskadon⁶ · Lili Zhao⁷ · Rosalynn M. Nazarian ⁸ · Alison B. Durham^{2,3} · Timothy M. Johnson^{2,3} · Aleodor A. Andea^{1,2,3} · Rajiv M. Patel ^{1,2,3} · Lori Lowe^{1,2,3} · Douglas R. Fullen^{1,2,3} · Noah A. Brown¹ · Scott A. Tomlins^{1,3,4,5} · Aaron M. Udager ^{1,4} · Paul W. Harms ^{1,2,3,4}

Received: 7 September 2019 / Revised: 24 October 2019 / Accepted: 31 October 2019 / Published online: 19 December 2019
© The Author(s), under exclusive licence to United States & Canadian Academy of Pathology 2019

Abstract

Microcystic adnexal carcinoma is a locally aggressive sweat gland carcinoma characterized by its infiltrative growth and histopathologic overlap with benign adnexal tumors, often posing challenges to both diagnosis and management. Understanding the molecular underpinnings of microcystic adnexal carcinoma may allow for more accurate diagnosis and identify potential targetable oncogenic drivers. We characterized 18 microcystic adnexal carcinomas by targeted, multiplexed PCR-based DNA next-generation sequencing of the coding sequence of over 400 cancer-relevant genes. The majority of cases had relatively few (<8) prioritized somatic mutations, and lacked an ultraviolet (UV) signature. The most recurrent mutation was *TP53* inactivation in four (22%) tumors. Frame-preserving insertions affecting the kinase domain of *JAK1* were detected in three (17%) cases, and were nonoverlapping with *TP53* mutations. Seven (39%) cases demonstrated copy number gain of at least one oncogene. By immunohistochemistry, p53 expression was significantly higher in microcystic adnexal carcinomas with *TP53* mutations compared with those without such mutations and syringomas. Similarly, phospho-STAT3 expression was significantly higher in microcystic adnexal carcinomas harboring *JAK1* kinase insertions compared with those with wild-type *JAK1* and syringomas. In conclusion, microcystic adnexal carcinomas are molecularly heterogeneous tumors, with inactivated p53 or activated JAK/STAT signaling in a subset. Unlike most other nonmelanoma skin cancers involving sun-exposed areas, most microcystic adnexal carcinomas lack evidence of UV damage, and hence likely originate from a relatively photo-protected progenitor population in the dermis. These findings have implications for the biology, diagnosis, and treatment of microcystic adnexal carcinomas, including potential for therapeutic targeting of p53 or the JAK/STAT pathway in advanced tumors.

Introduction

Microcystic adnexal carcinoma is a well-differentiated sweat gland carcinoma with a predilection for the face of

Supplementary information The online version of this article (<https://doi.org/10.1038/s41379-019-0424-4>) contains supplementary material, which is available to authorized users.

✉ May P. Chan
mpchan@med.umich.edu

✉ Paul W. Harms
paulharm@med.umich.edu

¹ Department of Pathology, Michigan Medicine, University of Michigan, Ann Arbor, MI, USA

² Department of Dermatology, Michigan Medicine, University of Michigan, Ann Arbor, MI, USA

³ Rogel Comprehensive Cancer Center, University of Michigan, Ann Arbor, MI, USA

⁴ Michigan Center for Translational Pathology, University of Michigan, Ann Arbor, MI, USA

⁵ Strata Oncology, Ann Arbor, MI, USA

⁶ Department of Urology, Vattikuti Urology Institute, Henry Ford Health System, Detroit, MI, USA

⁷ Department of Biostatistics, University of Michigan, Ann Arbor, MI, USA

⁸ Dermatopathology Unit, Department of Pathology, Massachusetts General Hospital, Harvard Medical School, Boston, MA, USA

elderly patients [1]. Although typically slow-growing and only rarely metastasizing [2–5], microcystic adnexal carcinoma is notorious for its locally aggressive growth, which may require radical and disfiguring surgical excision in order to achieve clear margins [6–8]. Furthermore, as its deeply infiltrative growth may be associated with minimal surface changes, the tumor may remain unrecognized for a prolonged period of time until critical structures are involved [9]. Microscopically, microcystic adnexal carcinoma is composed of infiltrating small ducts and cords of deceptively bland cells in a paucicellular or sclerotic stroma [10]. When superficially sampled, these features are often indistinguishable from those of a syringoma [11, 12]. Desmoplastic trichoepithelioma and morpheaform basal cell carcinoma also frequently enter the differential diagnosis [13–16]. Various immunohistochemical stains have been explored as potential discriminators of these entities, however, a definitively distinctive immunophenotype is lacking [15–17].

On a molecular level, very little is known regarding the genetic alterations occurring in microcystic adnexal carcinoma. In a recent case report, *TP53* mutation and copy number losses in *CDKN2A* and *CDKN2B* were identified in a metastatic microcystic adnexal carcinoma [5]. Another case demonstrated deletion of chromosome 6q by cytogenetic studies [18]. Other sweat gland carcinomas have been more systematically investigated for genetic changes. Among these are hidradenocarcinoma [19, 20], porocarcinoma [21–23], endocrine mucin-producing sweat gland carcinoma [24], aggressive digital papillary adenocarcinoma [25], as well as other eccrine and apocrine carcinomas. Some of the most common genetic changes reported in these tumors were *TP53* mutation, [21–23, 26] *EGFR* amplification [20] and mutation [22], and *HRAS* mutation [22]. Interestingly, *ERBB2* amplification was only a rare event in these carcinomas [19, 20, 27].

Given the significant challenges associated with the diagnosis and treatment of microcystic adnexal carcinoma, we aimed to identify recurrent genetic changes in a cohort of 18 microcystic adnexal carcinomas that may serve as diagnostic markers and/or potential targetable oncogenic drivers in these tumors.

Materials and methods

Case selection

This study was conducted according to previously approved Institutional Review Board protocols at the University of Michigan and Massachusetts General Hospital. The surgical pathology databases at these institutions were searched for “microcystic adnexal carcinoma” over 2001–2018 (University

of Michigan) and 2012–2017 (Massachusetts General Hospital). The original hematoxylin-eosin (H&E) stained slides were reviewed by two board-certified dermatopathologists (MPC and PWH) to confirm the diagnosis. Only cases with available formalin-fixed, paraffin-embedded tissue blocks containing adequate amount of tumor were selected.

Clinical and histopathologic review

Clinical data including patient’s age at diagnosis, sex, race, location of tumor, and follow-up data were obtained from electronic medical records. The H&E slides of each case were examined by MPC for the following features: keratin microcysts, squamous differentiation, follicular differentiation, solid component, involvement of subcutaneous fat and/or skeletal muscle, perineural invasion, angiotropism, tumor-associated inflammation, and prominent desmoplasia.

Targeted multiplexed PCR-based NGS

At least four 10- μ m-thick formalin-fixed paraffin-embedded sections were obtained from each tumor. Using H&E sections as a guide, the areas with highest tumor purity were macrodissected using a scalpel. DNA was isolated using the Qiagen Allprep formalin-fixed paraffin-embedded DNA/RNA Kit (Qiagen) and the Qiagen QIAcube (Qiagen) according to the manufacturer’s instructions, and were quantified using the Qubit 2.0 fluorometer (Life Technologies). Targeted multiplexed PCR (mxPCR)-based next-generation sequencing (NGS) was performed as previously described [28–30]. Forty nanograms of DNA per sample were used to generate libraries using the Ion AmpliSeq Library Kit 2.0 (Thermo Fisher Scientific) and targeted mxPCR with barcode incorporation using the Comprehensive Cancer Panel (CCP; Thermo Fisher Scientific), which targets 1,688,650 bases from 15,992 amplicons representing 409 cancer genes (Supplementary Table S1). Template preparation was performed using the Ion PI Hi-Q Template OT2 200 Kit (Thermo Fisher Scientific) and the Ion One-Touch ES Instrument (Thermo Fisher Scientific). Sequencing of templated libraries was then performed on an Ion Proton sequencer (Thermo Fisher Scientific) with Ion PI chips (Thermo Fisher Scientific) using the Ion PI Hi-Q Sequencing 200 Kit (Thermo Fisher Scientific) according to the manufacturer’s instructions.

Variant calling and prioritization

NGS data analysis was performed using Torrent Suite (version 5.0.4) and in-house previously-validated bioinformatics pipelines [31]. Sequencing reads were aligned with TMAP, and variant calling was performed using the variantCaller plugin. Annotated variants were filtered to

remove poorly supported calls, sequencing artifacts, and germline alterations. Variants present in the 1000 Genomes Projects, Exome Sequencing Project, and/or Exome Aggregation Consortium (ExAC) databases at population allele frequencies $>0.1\%$ were considered germline and excluded. Variants present in ExAC with a variant fraction between 40 and 60% or $>90\%$ were also excluded unless occurring at a well-supported somatic mutation hotspot in COSMIC (<https://cancer.sanger.ac.uk/cosmic>). Variants called in $>4\%$ of internally-sequenced samples using the same panel (CCP), as well as variants with extreme skewing of flow-corrected reads [$0.2 < (\text{FSAF}/\text{FSAR})$ or $(\text{FDP}/\text{DP}) > 5$], were also excluded. For all tumor samples, variants with flow-corrected variant allele containing reads counts (FAO) of <10 and flow-corrected read depth (FDP) of <50 were excluded; in addition, for tumor samples obtained prior to 2013, C→T and G→A variants were excluded if the FAO <15 . For tumor samples with an estimated tumor content $>20\%$, variants with an overall variant fraction (FAO/FDP) of $<10\%$ were excluded unless otherwise prioritized (see below for details); for tumor samples with an estimated tumor content $\leq 20\%$, variants with an overall variant fraction of $<5\%$ were excluded. High-confidence somatic variants passing the above criteria were visualized using the Integrated Genomics Viewer (Broad Institute) for read level confirmation. After filtering and visual confirmation, potential driving alterations were prioritized using the COSMIC database. Recurrent variants [including novel frame-preserving insertions/deletions (indels)] in known oncogenes and deleterious variants in established tumor suppressors were considered prioritized.

Copy number analysis

Amplicon-level read counts were determined using the coverageAnalysis plugin. Normalized, GC content-corrected read counts for each tumor sample were divided by the average of a pool of normal male tissue samples to generate amplicon-level copy number ratios, and weighted gene-level copy number estimates were determined as described previously [29, 32]. Genes with a log₂ copy number ratio estimate of <-1 or >0.80 were considered to have high-level loss (deletion) or gain (amplification), respectively.

UV signature analysis

Ultraviolet (UV) signature mutations were defined as C→T transitions at dipyrimidine sites (specifically, C→T transitions preceded by a 5' C or T). For samples with a predominance of C→T transitions, UV signature mutations were considered to be enriched if the ratio of these mutations to all C→T transitions significantly exceeded 0.5

(specifically, the lower bound of the 95% confidence interval calculated by the Clopper–Pearson approach was greater than 0.5). GraphPad Prism 7.00 software was used for this analysis.

Immunohistochemistry for p53 and phospho-STAT3

Four-micron-thick formalin-fixed paraffin-embedded sections were prepared from microcystic adnexal carcinoma cases with available tissue after NGS, and a cohort of 16 syringomas collected from University of Michigan Department of Pathology. These sections were immunostained with p53 and phospho-STAT3 antibodies according to the following protocols.

For p53, slides were deparaffinized, and heat-induced epitope retrieval was performed on the Ventana Benchmark Ultra immunostainer using a CC1 standard cell conditioning solution (Ventana Medical Systems) for 64 min. After blocking endogenous peroxidase activity, the slides were incubated for 32 min at 36 °C with a mouse monoclonal anti-p53 antibody (clone DO-7, predilute, Ventana) and subsequently detected by the Ultraview DAB detection system (Ventana).

For phospho-STAT3, slides were incubated at 60 °C for at least 2 h, and placed in EnVision FLEX Target Retrieval Solution, high pH (Agilent Dako) in a PT Link instrument (Agilent Dako) at 75 °C, heated to 97 °C for 20 min, and then cooled to 75 °C. Slides were then washed in 1× EnVision FLEX Wash Buffer (Agilent Dako), treated with Peroxidazed 1 (Biocare Medical), and Background Punisher (Biocare Medical). Rabbit monoclonal anti-STAT3 (phospho Y705) (clone EP2147Y, 1:200, Abcam) was added to each slide and incubated overnight at 4 °C, followed by a wash in 1× EnVision Wash Buffer and incubation in Mach2 Doublestain 1 (Biocare Medical). Slides were then treated with a Betazoid DAB solution (Biocare Medical), rinsed twice in distilled water, and treated with EnVision FLEX Hematoxylin (Agilent Dako).

Staining for each antibody was interpreted independently by MPC and PWH. For each case the staining intensity was graded (0 = negative, 1 = weak, 2 = moderate, and 3 = strong) and weighted by the percentage of cells with each intensity, giving rise to an h-score between 0 and 300. The averaged final h-score was calculated for each case. Scorers were blinded to mutation status; blinding was not possible for diagnosis (microcystic adnexal carcinoma vs. syringoma).

Statistical analysis

The microcystic adnexal carcinoma cases were divided into molecular subclasses based on NGS data. Clinical, histopathologic, and immunohistochemical findings were

compared between different subclasses and/or between microcystic adnexal carcinomas and syringomas using least squares mean test with Tukey–Cramer adjustment. A p value of <0.05 was considered statistically significant when comparing two groups (e.g., microcystic adnexal carcinomas with a particular mutation vs. microcystic adnexal carcinomas without the mutation). A more stringent p value cutoff of <0.01 was adopted when analyzing multiple subclasses (e.g., microcystic adnexal carcinomas with different genetic aberrations).

Results

Targeted NGS was performed on 20 microcystic adnexal carcinoma cases identified with sufficient formalin-fixed paraffin-embedded tissues, of which two were subsequently excluded due to poor DNA quality. The final cohort consisted of 18 microcystic adnexal carcinoma cases from 18 patients.

Clinical and histopathologic findings

The mean age of patients was 70 years (range, 31–93 years; median, 72 years). Half of the patients were women. Of the 15 patients whose race was known, one was African American and the rest were Caucasian. Fifteen (83%) tumors were located on the face; the remaining three tumors were located on the scalp, arm, and axilla. Follow-up data was available for 14 patients. None of these patients experienced local recurrence or metastasis over an average follow-up period of 27 months (range, 2–72 months; median, 24 months).

Histopathologically, all microcystic adnexal carcinomas displayed ductal differentiation with mild cytologic atypia and no to rare mitoses. Most (67%) microcystic adnexal carcinomas were deeply infiltrative tumors with involvement of skeletal muscles. A subset of cases displayed keratin microcysts (67%), squamous differentiation (67%), follicular differentiation (28%), and solid tumor nests (44%). Perineural invasion was found in 56% of cases, whereas angiotropism was seen in 17%. Tumor-associated inflammation ranged from minimal to moderate. Prominent desmoplasia was present in three (17%) cases. The clinical and histopathologic findings in all cases are listed in Table 1.

Tumor mutation burden and UV signature

Tumor purity of each sample was estimated on H&E sections and ranged from 10 to 80% (mean, 44%) (Supplementary Table S2). Targeted mxPCR NGS generated an average of 8,208,033 mapped reads yielding an average

depth of 525 \times (range: 270–800 \times) targeted base coverage (Supplementary Table S2). After stringent filtering, we identified an average of 12 high-confidence somatic mutations (range, 2–69) per sample, with the majority of cases harboring <8 mutations (Fig. 1a; Supplementary Table S3). On average, there was <1 high-confidence prioritized driving somatic mutation (range, 0–3) per sample.

One case (MAC-6) demonstrated the highest tumor mutation burden in this cohort with significant enrichment of UV signature mutations (Fig. 1a; Supplementary Table S3). The remaining 17 (94%) cases did not show a UV mutation signature. Interestingly, MAC-6 also coharbored *TP53* and *PTCH1* mutations (Supplementary Table S3); while these molecular changes raised suspicion for a basal cell carcinoma, re-review of the histopathologic features confirmed the diagnosis of microcystic adnexal carcinoma (Supplementary Fig. S1).

Recurrent prioritized mutations and protein expression

Two genes were found to be recurrently mutated after prioritization. Four (22%) cases harbored one or multiple inactivating missense mutations involving the *TP53* gene. The same mutations have been previously reported in a wide variety of human malignancies [33–43]. Immunohistochemistry for p53 performed on 13 microcystic adnexal carcinoma cases revealed overexpression in the mutant *TP53* subset relative to the wild-type subset (mean h-scores, 118 vs. 25; $p < 0.0001$) (Table 2; Fig. 2). Expression of p53 was also higher in the mutant microcystic adnexal carcinomas compared with syringomas (118 vs. 9; $p < 0.0001$) (Fig. 2). No significant difference was observed between microcystic adnexal carcinomas with wild-type *TP53* and syringomas ($p = 0.1410$) (Fig. 2).

Frame-preserving indel mutations in the *JAK1* gene were identified in three (17%) cases, confirmed by Sanger sequencing (data not shown). The insertions were located in the kinase domain of *JAK1* around its activation loop (Fig. 3a). Despite different indel events in MAC-7 and MAC-17, both resulted in the same amino acid change (P1044_V1045dup). The other indel event in MAC-2 resulted in E1012delinsDK, which is the precise amino acid position of the *JAK1* insertion previously reported in early T-cell precursor acute lymphoblastic leukemia (E1012insK) [44]. Immunohistochemistry for phospho-STAT3 revealed increased expression in the mutant *JAK1* microcystic adnexal carcinomas compared with the wild-type microcystic adnexal carcinomas (mean h-scores, 160 vs. 56; $p < 0.0001$) (Table 2) and syringomas (160 vs. 18; $p < 0.0001$) (Fig. 3b, c). Higher phospho-STAT3 expression was also observed in microcystic adnexal carcinomas with wild-type *JAK1* compared with syringomas (56 vs. 18; $p = 0.0047$) (Fig. 3b, c).

Table 1 Clinical and histopathologic findings of microcystic adnexal carcinomas (MACs).

Case	Age/sex	Race	Site	Clark level	Keratin microcysts	Squamous diff.	Follicular diff.	Solid component	PNI	Angiotropism	Inflammation ^b	Desmoplasia
MAC-1	67/M	C	Upper lip	V ^a	+	+	+	+	+	+	2	-
MAC-2	76/F	C	Eyebrow	V ^a	+	+	-	-	-	-	2	-
MAC-3	66/M	C	Scalp	V ^a	+	-	-	-	+	-	1	-
MAC-4	81/F	C	Arm	V	+	-	-	-	+	+	1	-
MAC-5	78/F	NK	Cheek	V ^a	+	+	+	+	+	-	1	-
MAC-6	69/M	NK	Lower lip	V ^a	+	+	-	-	+	-	2	+
MAC-7	56/M	C	Eyebrow	V ^a	-	-	+	+	+	-	2	-
MAC-8	75/F	C	Temple	V ^a	-	-	-	+	-	-	1	-
MAC-10	75/M	C	Lip/cheek	V ^a	+	+	-	+	+	-	1	-
MAC-11	62/M	C	Chin	V ^a	-	+	+	+	+	-	1	-
MAC-13	89/F	C	Cheek	V ^a	-	+	-	-	+	-	2	+
MAC-14	80/F	AA	Nose	IV	+	+	-	-	-	-	2	-
MAC-15	93/M	C	Nose (ala)	IV	+	+	-	+	-	-	1	-
MAC-16	65/M	C	Nose	IV	-	+	-	-	-	-	1	-
MAC-17	84/F	C	Nasolabial fold	V ^a	+	-	-	-	+	+	2	-
MAC-18	57/F	C	Upper lip	IV	+	+	-	-	-	-	1	-
MAC-20	55/M	C	Cheek	V ^a	-	+	+	+	-	-	1	-
MAC-21	31/F	NK	Axilla	V	+	-	-	-	-	-	2	+

AA African American, C Caucasian, *diff.* differentiation, F female, M male, NA not available, NK not known, PNI perineural invasion, + present, - absent

^aTumor infiltrated into skeletal muscle

^bInflammation was classified as: 1 = minimal, 2 = mild/moderate

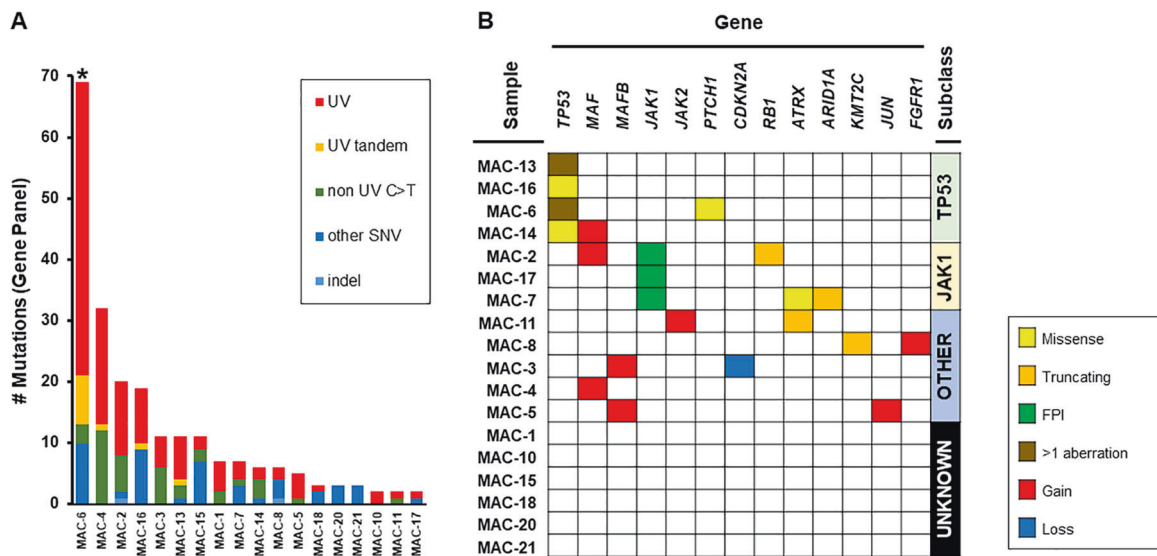


Fig. 1 Genomic changes in microcystic adnexal carcinomas (MACs). **a** Mutation burden across 409 cancer genes, by mutation type. In one case (MAC-6, marked by asterisk) a statistically significant UV signature was present. **b** Genomic alterations in MAC

suggest molecular subclasses. Truncating, Stop-gain or frameshift insertion. FPI, Frame-preserving indel. SNV, Single nucleotide variation.

Table 2 Immunohistochemical findings in different molecular subclasses of microcystic adnexal carcinomas (MACs).

Case	Tumor purity	Molecular subclass	p53 h-score	Phospho-STAT3 h-score
MAC-1	60%	Unknown	27.5	125
MAC-2	60%	JAK1	45	195
MAC-3	80%	Other	35	20
MAC-4	50%	Other	0	NA
MAC-5	40%	Other	12.5	80
MAC-6	20%	TP53	NA	NA
MAC-7	50%	JAK1	65	175
MAC-8	75%	Other	5	10
MAC-10	60%	Unknown	25	62.5
MAC-11	65%	Other	22.5	22.5
MAC-13	15%	TP53	175	80
MAC-14	15%	TP53	55	77.5
MAC-15	10%	Unknown	25	15
MAC-16	20%	TP53	125	65
MAC-17	40%	JAK1	7.5	110
MAC-18	50%	Unknown	NA	NA
MAC-20	40%	Unknown	NA	NA
MAC-21	35%	Unknown	NA	NA

Copy number alterations

Seven (39%) microcystic adnexal carcinoma cases demonstrated copy number gain of at least one of these oncogenes: *JAK2*, *MAF*, *MAFB*, *JUN*, and *FGFR1* (Fig. 1b; Supplementary Table S4). Only one case showed loss of *CDKN2A*.

Comparative analysis of molecular subclasses

Additional statistical analyses were performed after grouping the microcystic adnexal carcinoma cases into four molecular subclasses: (1) the “TP53” group harboring missense *TP53* mutations; (2) the “JAK1” group harboring frame-preserving *JAK1* mutations; (3) the “Other” group with amplification of other oncogenes (*JAK2*, *MAF*, *MAFB*, *JUN*, or *FGFR1*) without *JAK1* or *TP53* mutations; and (4) the “Unknown” group lacking any identifiable driver events (Table 2; Fig. 1b).

With regard to anatomic site, all subclasses occurred on the face, whereas tumors on sites other than the face were in the “Other” or “Unknown” subclass. Tumor mutation burden did not correlate with any molecular subclasses. The TP53 group was associated with a significantly lower mean tumor purity compared to all other groups ($p = 0.0028$); however, H&E re-review did not identify an explanation for this finding, as depth of invasion (Clark level) and tumor-associated inflammation were not significantly different compared with other groups. None of the other examined histopathologic features (keratin microcysts, squamous differentiation, follicular differentiation, solid component, involvement of subcutaneous fat and/or skeletal muscle, perineural invasion, angiotropism, tumor-associated inflammation, and prominent desmoplasia) were found to be associated with molecular subclasses. Hence, despite distinct genetic aberrations, different molecular subclasses of microcystic adnexal carcinoma are associated with similar tumor morphology and invasive characteristics.

Fig. 2 *TP53* mutations in microcystic adnexal carcinomas (MACs). **a** Representative p53 staining in MACs with and without *TP53* mutation and syringoma. **b** H-score quantitation of p53 staining by tumor type. Asterisks indicate statistically significant *p* values. MT, Mutant. WT, Wild-type.

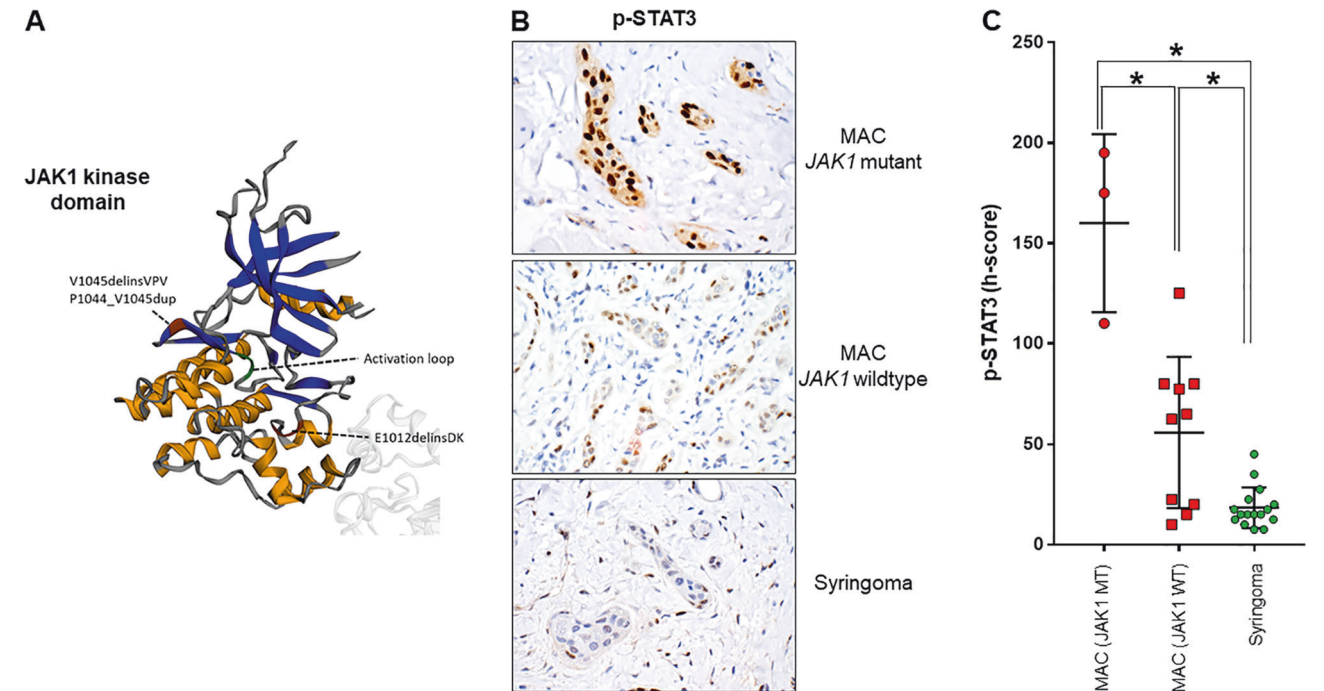
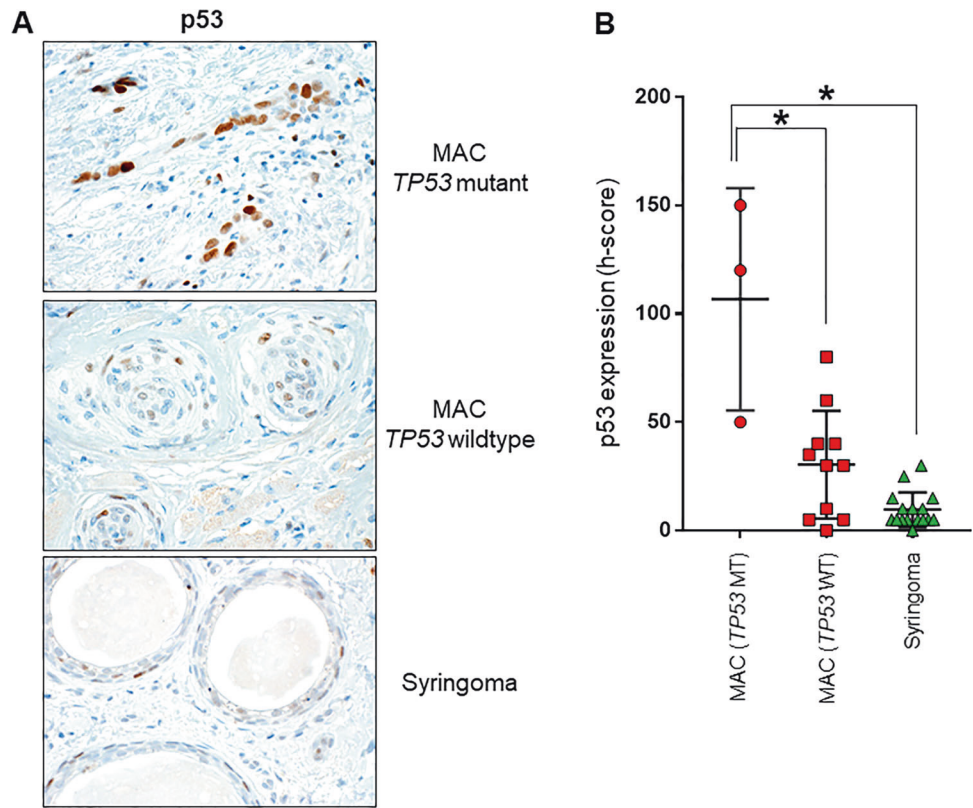


Fig. 3 *JAK1* mutations associated with *STAT3* activation in microcystic adnexal carcinomas (MACs). **a** In silico structure of *JAK1* kinase domain, demonstrating indels detected in MACs (red) adjacent to activation loop (green). **b** Representative phospho-*STAT3*

staining in MACs with and without *JAK1* mutation and syringoma. **c** H-score quantitation of phospho-*STAT3* staining by tumor type. Asterisks indicate statistically significant *p* values. MT, Mutant. WT, Wild-type.

Discussion

Diagnosis and treatment of microcystic adnexal carcinomas can be challenging, and understanding their molecular underpinnings may lead to improved management of these patients. Aside from a few case reports [5, 18], little is known regarding the genetic aberrations in microcystic adnexal carcinoma. We aimed to identify useful diagnostic markers and potentially targetable genetic changes in microcystic adnexal carcinoma. Using targeted mxPCR NGS, we were able to analyze 18 microcystic adnexal carcinoma samples for tumor mutation burden, UV mutational signature, driver mutations, and copy number variations. Expression of selected proteins was also evaluated by immunohistochemistry to identify potentially useful surrogate markers for the recurrent driver events in these tumors.

Mutational profiles of UV signature are characterized by high tumor mutation burden with a predominance of C→T transitions at dipyrimidine sites [45]. We have previously detected UV signature mutations in other skin tumors using the same sequencing approach employed in this study [46, 47]. Despite frequent involvement of sun-exposed skin, we found that most microcystic adnexal carcinomas had a low tumor mutation burden, and only one case (with *TP53* mutation) displayed statistically significant enrichment for UV signature mutations. While the low number of mutations hindered statistical power of this analysis for most of our samples, the low tumor mutation burden by itself represents indirect evidence for the absence of UV mutational signature. Overall, the lack of a UV signature in the vast majority of cases suggests that most microcystic adnexal carcinomas arise from a relatively sun-protected progenitor population in the deeper dermis, unlike most other nonmelanoma skin cancers frequently occurring on chronically sun-exposed skin [46, 48–50].

Inactivating mutations in *TP53* were found in 22% of our microcystic adnexal carcinoma cases. This frequency is relatively low compared with cutaneous squamous cell carcinoma and basal cell carcinoma, in which *TP53* was found to be mutated in up to 94% [51] and 61% [52] of cases, respectively. Other cutaneous carcinomas with frequent *TP53* mutations include virus-negative Merkel cell carcinoma (88%) [40] and porocarcinoma (67–80%) [22, 23]. As *TP53* mutations in cutaneous carcinomas are often UV-induced [23, 33], the absence of a UV mutational signature in the vast majority of microcystic adnexal carcinomas likely explains the relatively low frequency of *TP53* mutations in these cases. The wild-type *TP53* status of many microcystic adnexal carcinomas suggests potential susceptibility to therapy by MDM2 antagonists such as nutlin [53].

Most mutations in *TP53* result in more stable isoforms of the p53 protein than wild-type p53 [54, 55]. Overexpression

of p53, as shown by immunohistochemistry, thereby serves as a useful indicator of *TP53* mutation [56]. A previous study has demonstrated positive p53 staining in 23% of sweat gland carcinomas (not including microcystic adnexal carcinoma), whereas only 2% of benign sweat gland neoplasms expressed p53 [57]. As expected, microcystic adnexal carcinomas harboring *TP53* mutations were associated with significantly higher levels of p53 expression compared with those without *TP53* mutations and syringomas. Strong nuclear staining was noted in the majority of the tumor cells in *TP53*-mutated microcystic adnexal carcinomas. These findings support the use of p53 as a surrogate immunohistochemical marker for mutant p53, which may aid in distinguishing *TP53*-mutated microcystic adnexal carcinoma from syringoma in a partial biopsy.

Another recurrently mutated gene was *JAK1*, in which frame-preserving insertions were found in 17% of the microcystic adnexal carcinoma cases. Two of these resulted in the same amino acid change, while the other was previously reported in T-cell precursor acute lymphoblastic leukemia [44]. These insertions were located in the kinase domain around the activation loop. Interestingly, most of the known activating *JAK* mutations are located in the pseudokinase (inhibitory) domain, rather than the kinase domain itself [58–63]. We hypothesized that the *JAK1* insertions in microcystic adnexal carcinomas are also activating, either by directly increasing the catalytic activity of the kinase domain, or by blocking its interaction with the inhibitory domain. To test this hypothesis, we studied phospho-STAT3 expression in microcystic adnexal carcinomas and syringomas. Activated JAKs mediate phosphorylation of the STAT proteins and their translocation to the nucleus, resulting in downstream activation of oncogenes [64–66]. Demonstration of increased phospho-STAT3 (a usual partner of *JAK1*) by immunohistochemistry thereby supports an activated *JAK1*–STAT3 pathway. Indeed, we showed that microcystic adnexal carcinomas harboring *JAK1* mutations expressed significantly higher levels of phospho-STAT3 compared with those without the mutations, as well as syringomas. Together, these findings make for a strong argument that the *JAK1* mutations found in this cohort are functionally relevant. *JAK* inhibitors have been approved for management of certain myeloid neoplasms, and are in Phase 2 trials for the treatment of several types of carcinoma [67]. Our results suggest *JAK1* inhibition as a potential novel therapeutic approach for microcystic adnexal carcinomas with activation of this pathway.

The third molecular subclass demonstrated copy number gain of various oncogenes, namely *JAK2*, *MAF*, *MAFB*, *JUN*, and *FGFR1*. Amplification of *JAK2* has been described in triple-negative breast carcinoma [68, 69], gastric adenocarcinoma [70], nonsmall cell lung carcinoma [71], renal cell carcinoma [72], melanoma [73], as well as

lymphoma [74]. Interestingly, *JAK2* amplification often co-occurs with amplification of adjacent genes *PD-L1* and *PD-L2* on 9p24.1 [68–74], and hence is associated with high PD-L1 expression and possible enhanced response to anti-PD-1 immunotherapy [73]. The *MAF* and *MAFB* genes encode the c-Maf and MafB proteins, respectively. Amplification of *MAF* has been shown in breast carcinoma [75, 76], and amplification of *MAFB* in colorectal carcinoma [77]. Similarly, amplifications of *JUN* [78–80] and *FGFR1* [81–83] have been associated with various malignancies. Further studies are needed to better assess the incidence and potential prognostic and therapeutic implications of these oncogene amplifications in microcystic adnexal carcinoma.

In one-third of our cases no driver oncogenic events were identified. It is possible that these tumors may be driven by events not detectable by our targeted NGS approach, such as gene fusions. Gene fusions have been described in other cutaneous adnexal neoplasms. For example, cutaneous secretory carcinoma typically harbors *ETV6-NTRK3* gene fusion [84, 85], whereas hidradenoma is associated with *CRTC1-MAML2* or *CRTC3-MAML2* fusion [86, 87]. To identify potential gene fusions in microcystic adnexal carcinoma, a follow-up RNA sequencing study will be required.

Our study is limited by the relatively small number of cases. Some cases were excluded from this cohort due to low tumor purity, as the infiltrative cords and ducts in microcystic adnexal carcinoma are often separated by an ample amount of stroma as well as many pilosebaceous units on the face. Given the average sequencing depth (525×) relative to a minimum tumor percentage of 10%, we do not anticipate that significant mutations were missed by our approach. However, sample size may limit the power of our study for identifying significant differences between groups. As described above, although our panel is capable of detecting mutation and copy number change events in most genes with known relevance to cancer, a limitation of our approach is that some types of driver events, including gene fusions and promoter mutations/rearrangements, will not be detected. Another potential limitation is the lack of comparison to normal germline DNA, which may impact individual mutation calls and estimates of total mutational burden; however, our bioinformatics pipeline incorporates data from multiple large germline sequencing databases (see Materials and Methods for details) to reduce potential inclusion of germline variants. Finally, while copy number assessment by amplicon-based targeted NGS typically demonstrates high concordance with other more conventional methods (e.g., fluorescence in situ hybridization, chromosomal microarray, etc.) [32], low tumor content, and intratumoral heterogeneity may reduce the sensitivity of NGS-based approaches.

To our knowledge, this is the first report of the molecular changes in microcystic adnexal carcinomas using targeted NGS. Our results showed that microcystic adnexal carcinomas are genetically heterogeneous tumors, which may be grouped into several molecular subclasses based on a few recurrent driver events. We also demonstrated that high levels of p53 or phospho-STAT3 expression may support a diagnosis of microcystic adnexal carcinoma when syringoma is in the differential diagnosis. Lastly, the majority of microcystic adnexal carcinomas lack evidence of association with UV damage. Future studies should focus on assessment for gene fusions in the “unknown” molecular subclass, and the utility of additional immunohistochemical markers such as c-Maf, MafB, and PD-L1 (in relation to *JAK2* amplification) in aiding diagnosis and consideration for potential therapeutic options.

Acknowledgements This research was funded by the Anatomic Pathology Projects Committee, Department of Pathology, University of Michigan. We are grateful to Sharon Kerr and Threase Nickerson for administrative support.

Compliance with ethical standards

Conflict of interest SAT has had a prior sponsored research agreement with Thermo Fisher Scientific. SAT is a co-founder of, prior consultant to, equity holder in, and current employee of Strata Oncology. All other authors have no relevant conflicts of interest to disclose.

Publisher's note Springer Nature remains neutral with regard to jurisdictional claims in published maps and institutional affiliations.

References

1. King BJ, Tolkachjov SN, Winchester DS, Baum CL, Brewer JD, Arpey CJ, et al. Demographics and outcomes of microcystic adnexal carcinoma. *J Am Acad Dermatol*. 2018;79:756–8.
2. Carroll P, Goldstein GD, Brown CW. Metastatic microcystic adnexal carcinoma in an immunocompromised patient. *Dermatol Surg*. 2000;26:531–4.
3. Ban M, Sugie S, Kamiya H, Kitajima Y. Microcystic adnexal carcinoma with lymph node metastasis. *Dermatology*. 2003;207:395–7.
4. Yu JB, Blitzblau RC, Patel SC, Decker RH, Wilson LD. Surveillance, Epidemiology, and End Results (SEER) database analysis of microcystic adnexal carcinoma (sclerosing sweat duct carcinoma) of the skin. *Am J Clin Oncol*. 2010;33:125–7.
5. Chen MB, Laber DA. Metastatic microcystic adnexal carcinoma with DNA sequencing results and response to systemic anti-neoplastic chemotherapy. *Anticancer Res*. 2017;37:5109–11.
6. Bier-Laning CM, Hom DB, Gapany M, Manivel JC, Duvall AJ 3rd. Microcystic adnexal carcinoma: management options based on long-term follow-up. *Laryngoscope*. 1995;105:1197–201.
7. Frouin E, Vignon-Pennamen MD, Balme B, Cavelier-Balloy B, Zimmermann U, Ortonne N, et al. Anatomoclinical study of 30 cases of sclerosing sweat duct carcinomas (microcystic adnexal carcinoma, syringomatous carcinoma and squamoid eccrine ductal carcinoma). *J Eur Acad Dermatol Venereol*. 2015;29:1978–94.
8. Chaudhari SP, Mortazie MB, Blattner CM, Garelik J, Wolff M, Daulat J, et al. Treatments for microcystic adnexal carcinoma-A review. *J Dermatol Treat*. 2016;27:278–84.

9. Hamsch C, Hartschuh W. Microcystic adnexal carcinoma—aggressive infiltrative tumor often with innocent clinical appearance. *J Dtsch Dermatol Ges.* 2010;8:275–8.
10. Goldstein DJ, Barr RJ, Santa Cruz DJ. Microcystic adnexal carcinoma: a distinct clinicopathologic entity. *Cancer.* 1982;50:566–72.
11. Henner MS, Shapiro PE, Ritter JH, Leffell DJ, Wick MR. Solitary syringoma. Report of five cases and clinicopathologic comparison with microcystic adnexal carcinoma of the skin. *Am J Dermatopathol.* 1995;17:465–70.
12. Wallace JS, Bond JS, Seidel GD, Samie FH. An important mimicker: plaque-type syringoma mistakenly diagnosed as microcystic adnexal carcinoma. *Dermatol Surg.* 2014;40:810–2.
13. Ohtsuka H, Nagamatsu S. Microcystic adnexal carcinoma: review of 51 Japanese patients. *Dermatology.* 2002;204:190–3.
14. Kazakov DV, Kacerovska D, Michal M. Microcystic adnexal carcinoma with multiple areas of follicular differentiation toward germinative cells and specific follicular stroma (trichoblastomatous areas). *Am J Dermatopathol.* 2011;33:e47–9.
15. Tse JY, Nguyen AT, Le LP, Hoang MP. Microcystic adnexal carcinoma versus desmoplastic trichoepithelioma: a comparative study. *Am J Dermatopathol.* 2013;35:50–5.
16. Sellheyer K, Nelson P, Kutzner H, Patel RM. The immunohistochemical differential diagnosis of microcystic adnexal carcinoma, desmoplastic trichoepithelioma and morpheaform basal cell carcinoma using BerEP4 and stem cell markers. *J Cutan Pathol.* 2013;40:363–70.
17. Hoang MP, Dresser KA, Kapur P, High WA, Mahalingam M. Microcystic adnexal carcinoma: an immunohistochemical reappraisal. *Mod Pathol.* 2008;21:178–85.
18. Wohlfahrt C, Ternesten A, Sahlin P, Islam Q, Stenman G. Cytogenetic and fluorescence in situ hybridization analyses of a microcystic adnexal carcinoma with del(6)(q23q25). *Cancer Genet Cytogenet.* 1997;98:106–10.
19. Kazakov DV, Ivan D, Kutzner H, Spagnolo DV, Grossmann P, Vanecek T, et al. Cutaneous hidradenocarcinoma: a clinicopathological, immunohistochemical, and molecular biologic study of 14 cases, including Her2/neu gene expression/amplification, TP53 gene mutation analysis, and t(11;19) translocation. *Am J Dermatopathol.* 2009;31:236–47.
20. Le LP, Dias-Santagata D, Pawlak AC, Cospoer AK, Nguyen AT, Selim MA, et al. Apocrine-ecrine carcinomas: molecular and immunohistochemical analyses. *PLoS ONE.* 2012;7:e47290.
21. Takata M, Hashimoto K, Mehregan P, Lee MW, Yamamoto A, Mohri S. Genetic changes in sweat gland carcinomas. *J Cutan Pathol.* 2000;27:30–5.
22. Harms PW, Hovelson DH, Cani AK, Omata K, Haller MJ, Wang ML, et al. Porocarcinomas harbor recurrent HRAS-activating mutations and tumor suppressor inactivating mutations. *Hum Pathol.* 2016;51:25–31.
23. Botic M, Kirchner M, Brasanac D, Leichsenring J, Lier A, Volckmar AL, et al. Targeted molecular profiling reveals genetic heterogeneity of poromas and porocarcinomas. *Pathology.* 2018;50:327–32.
24. Qin H, Moore RF, Ho CY, Eshleman J, Eberhart CG, Cuda J. Endocrine mucin-producing sweat gland carcinoma: a study of 11 cases with molecular analysis. *J Cutan Pathol.* 2018. <https://doi.org/10.1111/cup.13308>.
25. Bell D, Aung P, Prieto VG, Ivan D. Next-generation sequencing reveals rare genomic alterations in aggressive digital papillary adenocarcinoma. *Ann Diagn Pathol.* 2015;19:381–4.
26. Biernat W, Peraud A, Wozniak L, Ohgaki H. p53 mutations in sweat gland carcinomas. *Int J Cancer.* 1998;76:317–20.
27. Dias-Santagata D, Lam Q, Bergethon K, Baker GM, Iafrate AJ, Rakheja D, et al. A potential role for targeted therapy in a subset of metastasizing adnexal carcinomas. *Mod Pathol.* 2011;24:974–82.
28. Hovelson DH, McDaniel AS, Cani AK, Johnson B, Rhodes K, Williams PD, et al. Development and validation of a scalable next-generation sequencing system for assessing relevant somatic variants in solid tumors. *Neoplasia.* 2015;17:385–99.
29. Cani AK, Hovelson DH, McDaniel AS, Sadis S, Haller MJ, Yadati V, et al. Next-gen sequencing exposes frequent MED12 mutations and actionable therapeutic targets in phyllodes tumors. *Mol Cancer Res.* 2015;13:613–9.
30. Warrick JI, Hovelson DH, Amin A, Liu CJ, Cani AK, McDaniel AS, et al. Tumor evolution and progression in multifocal and paired non-invasive/invasive urothelial carcinoma. *Virchows Arch.* 2015;466:297–311.
31. Cani AK, Soliman M, Hovelson DH, Liu CJ, McDaniel AS, Haller MJ, et al. Comprehensive genomic profiling of orbital and ocular adnexal lymphomas identifies frequent alterations in MYD88 and chromatin modifiers: new routes to targeted therapies. *Mod Pathol.* 2016;29:685–97.
32. Grasso C, Butler T, Rhodes K, Quist M, Neff TL, Moore S, et al. Assessing copy number alterations in targeted, amplicon-based next-generation sequencing data. *J Mol Diagn.* 2015;17:53–63.
33. Ziegler A, Leffell DJ, Kunala S, Sharma HW, Gailani M, Simon JA, et al. Mutation hotspots due to sunlight in the p53 gene of non-melanoma skin cancers. *Proc Natl Acad Sci USA.* 1993;90:4216–20.
34. Reichel MB, Ohgaki H, Petersen I, Kleihues P. p53 mutations in primary human lung tumors and their metastases. *Mol Carcinog.* 1994;9:105–9.
35. Gaidano G, Volpe G, Pastore C, Chiarle R, Capello D, Ghoghini A, et al. Detection of BCL-6 rearrangements and p53 mutations in Malt-lymphomas. *Am J Hematol.* 1997;56:206–13.
36. Biramijamal F, Allameh A, Mirbod P, Groene HJ, Koomagi R, Hollstein M. Unusual profile and high prevalence of p53 mutations in esophageal squamous cell carcinomas from northern Iran. *Cancer Res.* 2001;61:3119–23.
37. Burger PC, Minn AY, Smith JS, Borell TJ, Jedlicka AE, Huntley BK, et al. Losses of chromosomal arms 1p and 19q in the diagnosis of oligodendroglioma. A study of paraffin-embedded sections. *Mod Pathol.* 2001;14:842–53.
38. Jones S, Zhang X, Parsons DW, Lin JC, Leary RJ, Angenendt P, et al. Core signaling pathways in human pancreatic cancers revealed by global genomic analyses. *Science.* 2008;321:1801–6.
39. Stephens PJ, Tarpey PS, Davies H, Van Loo P, Greenman C, Wedge DC, et al. The landscape of cancer genes and mutational processes in breast cancer. *Nature.* 2012;486:400–4.
40. Harms PW, Vats P, Verhaegen ME, Robinson DR, Wu YM, Dhanasekaran SM, et al. The distinctive mutational spectra of polyomavirus-negative Merkel cell carcinoma. *Cancer Res.* 2015;75:3720–7.
41. van de Wetering M, Francies HE, Francis JM, Bounova G, Iorio F, Pronk A, et al. Prospective derivation of a living organoid biobank of colorectal cancer patients. *Cell.* 2015;161:933–45.
42. De Luca F, Rotunno G, Salvianti F, Galardi F, Pestrin M, Gabellini S, et al. Mutational analysis of single circulating tumor cells by next generation sequencing in metastatic breast cancer. *Oncotarget.* 2016;7:26107–19.
43. Zehir A, Benayed R, Shah RH, Syed A, Middha S, Kim HR, et al. Mutational landscape of metastatic cancer revealed from prospective clinical sequencing of 10,000 patients. *Nat Med.* 2017;23:703–13.
44. Zhang J, Ding L, Holmfeldt L, Wu G, Heatley SL, Payne-Turner D, et al. The genetic basis of early T-cell precursor acute lymphoblastic leukaemia. *Nature.* 2012;481:157–63.
45. Brash DE. UV signature mutations. *Photochem Photobiol.* 2015;91:15–26.
46. Harms PW, Collie AM, Hovelson DH, Cani AK, Verhaegen ME, Patel RM, et al. Next generation sequencing of Cytokeratin 20-negative Merkel cell carcinoma reveals ultraviolet-signature

- mutations and recurrent TP53 and RB1 inactivation. *Mod Pathol.* 2016;29:240–8.
47. Harms KL, Lazo de la Vega L, Hovelson DH, Rahrig S, Cani AK, Liu CJ, et al. Molecular profiling of multiple primary Merkel cell carcinoma to distinguish genetically distinct tumors from clonally related metastases. *JAMA Dermatol.* 2017;153:505–12.
 48. Rass K, Reichrath J. UV damage and DNA repair in malignant melanoma and nonmelanoma skin cancer. *Adv Exp Med Biol.* 2008;624:162–78.
 49. Jayaraman SS, Rayhan DJ, Hazany S, Kolodney MS. Mutational landscape of basal cell carcinomas by whole-exome sequencing. *J Invest Dermatol.* 2014;134:213–20.
 50. Chan JW, Yeh I, El-Sayed IH, Algazi AP, Glastonbury CM, Ha PK, et al. Ultraviolet light-related DNA damage mutation signature distinguishes cutaneous from mucosal or other origin for head and neck squamous cell carcinoma of unknown primary site. *Head Neck.* 2019;41:E82–5.
 51. Pickering CR, Zhou JH, Lee JJ, Drummond JA, Peng SA, Saade RE, et al. Mutational landscape of aggressive cutaneous squamous cell carcinoma. *Clin Cancer Res.* 2014;20:6582–92.
 52. Bonilla X, Parmentier L, King B, Bezrukov F, Kaya G, Zoete V, et al. Genomic analysis identifies new drivers and progression pathways in skin basal cell carcinoma. *Nat Genet.* 2016;48:398–406.
 53. Shen H, Maki CG. Pharmacologic activation of p53 by small-molecule MDM2 antagonists. *Curr Pharm Des.* 2011;17:560–8.
 54. Midgley CA, Lane DP. p53 protein stability in tumour cells is not determined by mutation but is dependent on Mdm2 binding. *Oncogene.* 1997;15:1179–89.
 55. Vijayakumaran R, Tan KH, Miranda PJ, Haupt S, Haupt Y. Regulation of mutant p53 protein expression. *Front Oncol.* 2015;5:284.
 56. Bartek J, Bartkova J, Vojtesek B, Lane D. Aberrant expression of the p53 oncoprotein is a common feature of a wide spectrum of human malignancies. *Oncogene.* 1991;6:1699–703.
 57. Wienecke R, Eckert F, Kaudewitz P, de Viragh PA, Heidl G, Volkenandt M. p53 protein in benign and malignant sweat gland tumors. *Am J Dermatopathol.* 1994;16:126–9.
 58. Baxter EJ, Scott LM, Campbell PJ, East C, Fourouclas N, Swanton S, et al. Acquired mutation of the tyrosine kinase JAK2 in human myeloproliferative disorders. *Lancet.* 2005;365:1054–61.
 59. James C, Ugo V, Le Couedic JP, Staerk J, Delhommeau F, Lacout C, et al. A unique clonal JAK2 mutation leading to constitutive signalling causes polycythaemia vera. *Nature.* 2005;434:1144–8.
 60. Kralovics R, Passamonti F, Buser AS, Teo SS, Tiedt R, Passweg JR, et al. A gain-of-function mutation of JAK2 in myeloproliferative disorders. *N Engl J Med.* 2005;352:1779–90.
 61. Levine RL, Wadleigh M, Cools J, Ebert BL, Wernig G, Huntly BJ, et al. Activating mutation in the tyrosine kinase JAK2 in polycythemia vera, essential thrombocythemia, and myeloid metaplasia with myelofibrosis. *Cancer Cell.* 2005;7:387–97.
 62. Flex E, Petrangeli V, Stella L, Chiaretti S, Hornakova T, Knoops L, et al. Somatically acquired JAK1 mutations in adult acute lymphoblastic leukemia. *J Exp Med.* 2008;205:751–8.
 63. Vainchenker W, Constantinescu SN. JAK/STAT signaling in hematological malignancies. *Oncogene.* 2013;32:2601–13.
 64. Ihle JN. STATs: signal transducers and activators of transcription. *Cell.* 1996;84:331–4.
 65. Leonard WJ. STATs and cytokine specificity. *Nat Med.* 1996;2:968–9.
 66. Imada KI, Leonard WJ. The Jak-STAT pathway. *Mol Immunol.* 2000;37:1–11.
 67. Vainchenker W, Leroy E, Gilles L, Marty C, Plo I, Constantinescu SN. JAK inhibitors for the treatment of myeloproliferative neoplasms and other disorders. *F1000Res.* 2018;7:82.
 68. Barrett MT, Anderson KS, Lenkiewicz E, Andreozzi M, Cunliffe HE, Klassen CL, et al. Genomic amplification of 9p24.1 targeting JAK2, PD-L1, and PD-L2 is enriched in high-risk triple negative breast cancer. *Oncotarget.* 2015;6:26483–93.
 69. Balko JM, Schwarz LJ, Luo N, Estrada MV, Giltneane JM, Dávila-González D, et al. Triple-negative breast cancers with amplification of JAK2 at the 9p24 locus demonstrate JAK2-specific dependence. *Sci Transl Med.* 2016;8:334ra53.
 70. Cancer Genome Atlas Research Network. Comprehensive molecular characterization of gastric adenocarcinoma. *Nature.* 2014;513:202–9.
 71. Clavé S, Pijuan L, Casadevall D, Taus Á, Gimeno J, Hernández-Llodrà S, et al. CD274 (PDL1) and JAK2 genomic amplifications in pulmonary squamous-cell and adenocarcinoma patients. *Histopathology.* 2018;72:259–69.
 72. Gupta S, Cheville JC, Jungbluth AA, Zhang Y, Zhang L, Chen YB, et al. JAK2/PD-L1/PD-L2 (9p24.1) amplifications in renal cell carcinomas with sarcomatoid transformation: implications for clinical management. *Mod Pathol.* 2019;32:1344–58.
 73. Gupta S, Vanderbilt CM, Cotzia P, Arias Stella JA 3rd, Chang JC, Chen Y, et al. JAK2, PD-L1, and PD-L2 (9p24.1) amplification in metastatic mucosal and cutaneous melanomas with durable response to immunotherapy. *Hum Pathol.* 2019;88:87–91.
 74. Van Roosbroeck K, Ferreiro JF, Tousseyn T, van der Krogt JA, Michaux L, Pienkowska-et al. Genomic alterations of the JAK2 and PDL loci occur in a broad spectrum of lymphoid malignancies. *Genes Chromosom Cancer.* 2016;55:428–41.
 75. Pavlovic M, Arnal-Estapé A, Rojo F, Bellmunt A, Tarragona M, Guiu M, et al. Enhanced MAF oncogene expression and breast cancer bone metastasis. *J Natl Cancer Inst.* 2015;107:djv256.
 76. Coleman R, Hall A, Albanell J, Hanby A, Bell R, Cameron D, et al. Effect of MAF amplification on treatment outcomes with adjuvant zoledronic acid in early breast cancer: a secondary analysis of the international, open-label, randomised, controlled, phase 3 AZURE (BIG 01/04) trial. *Lancet Oncol.* 2017;18:1543–52.
 77. Yang LS, Zhang XJ, Xie YY, Sun XJ, Zhao R, Huang QH. SUMOylated MAFB promotes colorectal cancer tumorigenesis. *Oncotarget.* 2016;7:83488–501.
 78. Taniguchi T, Karnan S, Fukui T, Yokoyama T, Tagawa H, Yokoi K, et al. Genomic profiling of malignant pleural mesothelioma with array-based comparative genomic hybridization shows frequent non-random chromosomal alteration regions including JUN amplification on 1p32. *Cancer Sci.* 2007;98:438–46.
 79. Mariani O, Brennetot C, Coindre JM, Gruel N, Ganem C, Delattre O, et al. JUN oncogene amplification and overexpression block adipocytic differentiation in highly aggressive sarcomas. *Cancer Cell.* 2007;11:361–74.
 80. Saâda-Bouaid E, Burel-Vandenbos F, Ranchère-Vince D, Birtwisle-Peyrottes I, Chetaille B, Bouvier C, et al. Prognostic value of HMG2A, CDK4, and JUN amplification in well-differentiated and dedifferentiated liposarcomas. *Mod Pathol.* 2015;28:1404–14.
 81. von Loga K, Kohlhaussen J, Burkhardt L, Simon R, Steurer S, Burdak-Rothkamm S, et al. FGFR1 amplification is often homogeneous and strongly linked to the squamous cell carcinoma subtype in esophageal carcinoma. *PLoS ONE.* 2015;10:e0141867.
 82. Sousa V, Reis D, Silva M, Alarcão AM, Ladeirinha AF, d'Aguiar MJ, et al. Amplification of FGFR1 gene and expression of FGFR1 protein is found in different histological types of lung carcinoma. *Virchows Arch.* 2016;469:173–82.
 83. Clauditz TS, Böttcher A, Hanken H, Borgmann K, Sauter G, Wilczak W, et al. Prevalence of fibroblast growth factor receptor 1 (FGFR1) amplification in squamous cell carcinomas of the head and neck. *J Cancer Res Clin Oncol.* 2018;144:53–61.

84. Bishop JA, Taube JM, Su A, Binder SW, Kazakov DV, Michal M, et al. Secretory carcinoma of the skin harboring ETV6 gene fusions: a cutaneous analogue to secretory carcinomas of the breast and salivary glands. *Am J Surg Pathol.* 2017;41:62–6.
85. Kastnerova L, Luzar B, Goto K, Grishakov V, Gatalica Z, Kamarachev J, et al. Secretory carcinoma of the skin: Report of 6 cases, including a case with a novel NF1X-PKN1 translocation. *Am J Surg Pathol.* 2019;43:1092–8.
86. Kyrpychova L, Kacerovska D, Vanecek T, Grossmann P, Michal M, Kerl K, et al. Cutaneous hidradenoma: a study of 21 neoplasms revealing neither correlation between the cellular composition and CRTC1-MAML2 fusions nor presence of CRTC3-MAML2 fusions. *Ann Diagn Pathol.* 2016;23:8–13.
87. Kuma Y, Yamada Y, Yamamoto H, Kohashi K, Ito T, Furue M, et al. A novel fusion gene CRTC3-MAML2 in hidradenoma: histopathological significance. *Hum Pathol.* 2017;70:55–61.